

Biosynthesis, Characterization, Adsorption and Antimicrobial studies of Vanadium Oxide Nanoparticles Using Punica Granatum Extract

Angham Tariq Ali *  , Lekaa K. Abdul Kareem  

Department of Chemistry, College of Education for Pure Sciences (Ibn Al-Haitham), University of Baghdad, Baghdad, Iraq.

*Corresponding Author.

Received 15/11/2022, Revised 17/02/2023, Accepted 19/02/2023, Published Online First 20/07/2023, Published 01/02/2024



© 2022 The Author(s). Published by College of Science for Women, University of Baghdad.

This is an Open Access article distributed under the terms of the [Creative Commons Attribution 4.0 International License](https://creativecommons.org/licenses/by/4.0/), which permits unrestricted use, distribution, and reproduction in any medium, provided the original work is properly cited.

Abstract

This study includes using green or biosynthesis-friendly technology, which is effective in terms of low cost and low time and energy to prepare V_2O_5 NPs nanoparticles from vanadium sulfate $VSO_4 \cdot H_2O$ using aqueous extract of Punica Granatum at a concentration of 0.1M and with a basic medium $PH=8-12$. The V_2O_5 NPs nanoparticles were diagnosed using several techniques, such as FT-IR, UV-visible with energy gap $E_g = 3.734eV$, and the X-Ray diffraction XRD was calculated using the Debye Scherrer equation. It was discovered to be 34.39nm, Scanning Electron Microscope (SEM), Transmission Electron Microscopy TEM. The size, structure, and composition of synthetic V_2O_5 NPs were determined using the (EDX) pattern, Atomic force microscopy AFM. The adsorption experiment was successfully conducted on metal ions M (II), such as Co, Ni, and Cu. The results proved removal simultaneously from water using V_2O_5 NPs based on surface shape on the affinity of three metal ions. The adsorption rate of Ni(II) is the highest one in the time scale and conditions of our experiment at all surfaces, while Co(II) and Cu(II) ions are close in magnitude. The removal efficiencies of mixed ($M^{+2} = Co, Ni, \text{ and } Cu$) ions with λ_{max} for Co, Ni, and Cu ions are 510,425 and 814 nm 56.66%, 77.00%, and 27.23%, respectively. The Antimicrobial activity of V_2O_5 NPs in three concentrations, 25%, 50%, and 75%, was tested against *Escherichia coli*, *Staphylococcus aureus*, and *Candida albicans* fungus. The results of the inhibition of vanadium oxide nanoparticles against positive and negative bacteria were compared with the standard drug Amoxicillin and the results of fungus inhibition with the standard drug Metronidazole. It was found that nano-oxide is more effective at 75% concentration.

Keywords: Adsorption, Antimicrobial, Biosynthesis, Punica Granatum, Removal.

Introduction

For the development of green technology, science and technology are developing at the fastest rate. One of the fascinating fields that produce and use

materials with interatomic structural properties is nanotechnology¹. In the 21st century, nanotechnology has become a significant scientific

advancement. Nanoparticles are described as particles with a size between 1 -100 nm and having dimensions measured in billionths of a meter². Nanoparticles are cutting-edge scientific and technological materials with several uses in agriculture, medicine, electronics, chemicals, and pharmaceuticals³. One of the fundamental goals in chemistry is to biosynthesize nanoparticles with desired morphology (shape, size, and crystalline nature), which can be used for various applications, including catalysis, biomedical, cheaper electrode, and biosensor⁴. Besides their distinct chemical and physical characteristics, nanoparticles functioned as a link between bulk materials and molecule or atomic structure⁵. As a result, they are the finest choice for many crucial applications, including biotechnology, trace substance identification, medicine, and electrochemistry. Vanadium pentoxide (V_2O_5) has recently seen an increase in interest as a semiconductor for solar cells, batteries, and gas sensing⁶. Bactericidal properties of metal oxide nanoparticles have been established. They can be used as suspensions for wastewater treatment and to prepare practical application surfaces⁷. The antibacterial mechanisms of metal oxide nanoparticles such as CuO, ZnO, MgO, TiO₂, and

CeO₂ have been extensively researched because of their widespread application. Although the release of soluble ions is responsible for the antibacterial action of metal nanoparticles⁸, the mechanism of metal oxide nanoparticles can be very different. By producing reactive oxygen species (ROS) and destroying the genetic material, CuO destroys bacteria⁹. As a result of heavy contamination from industrial/agricultural effluents and artificial pollution risks, many developing countries have faced significant issues in ensuring a sustainable drinking water supply for their populations in recent years¹⁰. Innovative treatment methods based on technology are necessary for a sustainable drinking water supply. The ideal choice for futuristic adsorbents to remove water toxins is nano-sized metal oxides since these substances have the qualities of simplicity, adaptability, efficacy, and high surface reactivity¹¹. In the present study, we have developed a facile green synthesis method for preparing V₂O₅NPs using Punica Granatum extract. The objective of this research was to achieve the goals of green synthesis for potential application and antibacterial activity used as an adsorbent to metal ions.

Materials and Methods

Collection of sample a local source of Punica granatum collected and marked. Hydrated vanadium sulfate is used $VOSO_4 \cdot H_2O$ were acquired from England, NaOH from Alpha India's Alpha Chemical, ethanol from sakma aldaraj, copper, cobalt, and Nickel sulfate. All compounds are used. To create and identify the compounds, various spectroscopic and microscopic techniques were applied, following a Centrifuge type PLC, a Magnetic Stirrer, a Sensitive Electronic Balance type RADWAG, model As 220C1, and an Electric Oven type (FAITHFUL) model -WHL. 25 AB and a Shaking Water Bath type (SCL FINETEDI), PH-type UV-visible tape measure (160/Uv) Shimadzu, FT-IR (8500S) type spectroscopy, X-ray (XRD) diffraction type PW1730 (Phillips/ Holland) were examined in the laboratories of the (center of examinations). SEM type FESEM-EDS Model MIRAI, manufacturer TESCAN and country of manufacture Czech, Application of an X-ray energy

dispersion device (EDX).TEM with the model number EM10C-100Kv. AFM, the magnitude of the zeta potential.

Preparation of Punica Granatum extract

A Fresh pomegranate peel has been gathered and cleaned with deionized water to remove dust particles. The dry pomegranate peel is gently combined in a mixer to create homogenous powders. Then, 20 g of leaves were pulverized and mixed with 200 ml of deionized water, then heated for 30 minutes at 90 °C with stirring. The solution was filtered and stored in the fridge.

Preparation of V₂O₅ NPs

The biosynthesis technique was used to synthesize vanadium oxide (V_2O_5) nanoparticles. Accordingly, 100 ml of pomegranate peel extract was added slowly (one drop per second) to 0.012 moles, 50 ml of $VOSO_4 \cdot H_2O$, and stirred for 30 minutes. Then, 40 ml of 1 N NaOH was added to

the solution. The pH value turned to 12. A dark green precipitate was obtained; the precipitate was washed with deionized water (all steps done with a centrifuge, then decantation). Then, it dried for four h at 110 °C in the oven and then calcined for four h at 300 °C. A yellowish powder of vanadium oxide nanoparticles was obtained.

Study of Adsorption

A stock solution was made by dissolving 10g of $\text{CoCl}_2 \cdot 6\text{H}_2\text{O}$ in one Liter of distilled water to get 10000 ppm. For $\text{NiCl}_2 \cdot 4\text{H}_2\text{O}$ and $\text{CuCl}_2 \cdot 2\text{H}_2\text{O}$, the stock was prepared by dissolving 5g in one Liter of distilled water. Hence the stock concentration was 5000 ppm for each.

Adsorption Process

Adsorption kinetics was carried out by putting 0.1 gm of the adsorbent nanoparticle into 50 ml of

the 1000 ppm metal ion solution in the shaker water bath at 30°C and shaking rate 150 rpm; the adsorbent was separated from the solution at definite times by centrifuging then decantation, the remaining clear solution was measured by visible spectrophotometer to determine the remaining concentration after adsorption using the calibration curve.

Biological Activity

The disc diffusion method in a nutrient medium (jellose medium) type Muller Hinton agar was used to test the antimicrobial activity of the synthetic V_2O_5 NPs against two reference bacterial strains, (G+) *Staphylococcus aureus* and (G-) *Escherichia coli*, as well as *Candida albicans* fungal. The same method was used to test the antifungal activity using the nutrient medium (agar) potato dextrose.

Results and Discussion

FT-IR spectrum analysis

FT-IR spectrum analysis was performed on the vanadium oxide Fig.1. The characteristic V_2O_5 peaks were located at 1026.13 cm^{-1} and 825 cm^{-1} , respectively. These values correspond to the

stretching vibration of terminal oxygen bonds, $\text{V}=\text{O}$ (825 cm^{-1}), and the vibration of doubly coordinated oxygen (bridge oxygen) bonds, $\text{V}-\text{O}-\text{V}$ (1038 cm^{-1}). Both bands at 597.94 and 420.48 cm^{-1} were brought about by the $\text{V}-\text{O}$ stretching mode¹².

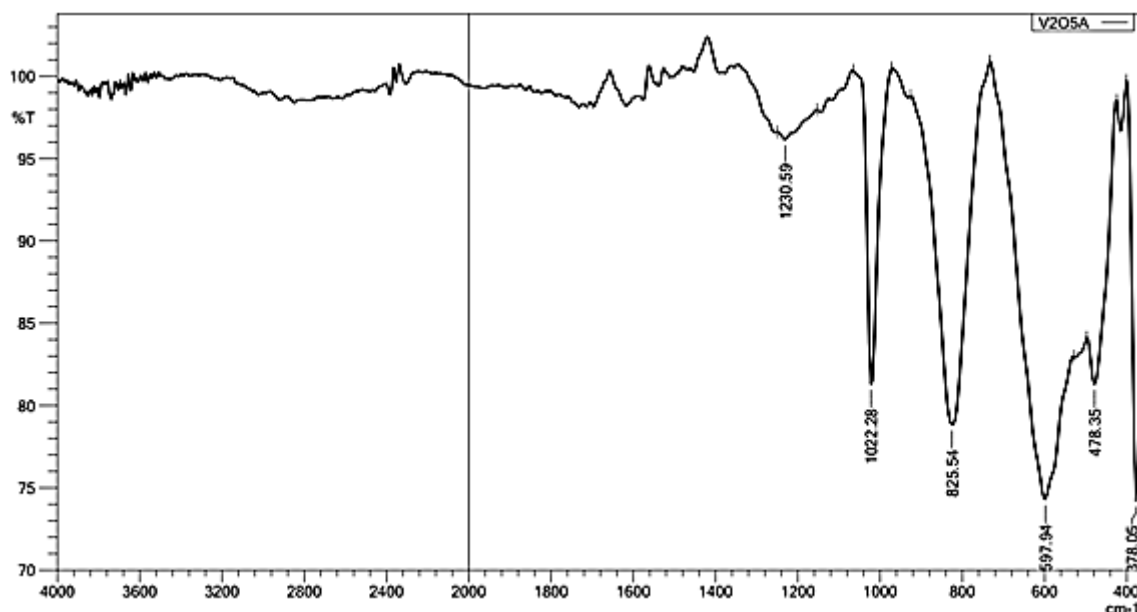


Figure 1. FT-IR spectrum of V_2O_5 NPs.

UV-Visible

The UV-Visible spectrum was used to investigate the prepared V_2O_5 Nps optical characteristics. Fig. 2 shows the UV-Vis absorption spectrum of the

biosynthesis V_2O_5 Nps dissolved in deionized water. The transition holes process between V and O caused the absorption peak to appear in this spectrum at 332 nm, as a bonus, the quantum

confinement property. The energy gap was calculated using the equation $E_g = 1239.83 / \lambda$ and was 3.7344 eV.

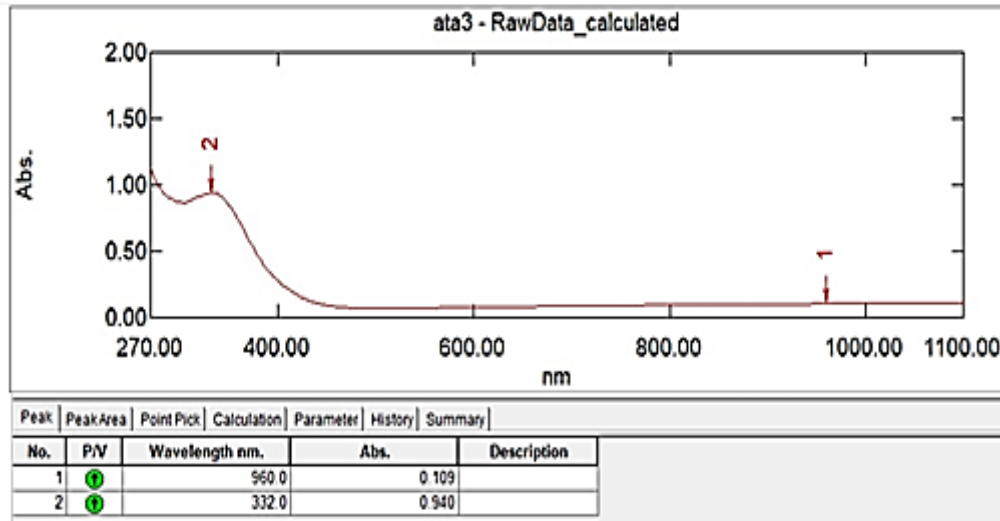


Figure 2. UV-Visible spectrum of V₂O₅Nps.

XRD

XRD measurements confirmed the structure, crystallinity, and phase of the crystals produced at 300 °C, as shown in Fig. 3. According to XRD analysis, orthorhombic V₂O₅ consistent with the standard JCPDS data card no: 01-070-8747, planes 200, 001, 101, 110, 400, 011, 310, 002, 411 and 600 are allocated to a series of diffraction peaks at 2θ of

15.5, 20.4, 21.8, 25.6, 31.1, 32.4, 34.3, 42.1, 45.6, and 51.2, respectively. XRD measurements confirm the creation of extremely crystalline V₂O₅ samples by the biosynthesis method because no impurity peaks were seen. The numbers in the JCPDS data correspond to the predicted crystallite size of the unit cell volume Table 1¹³.

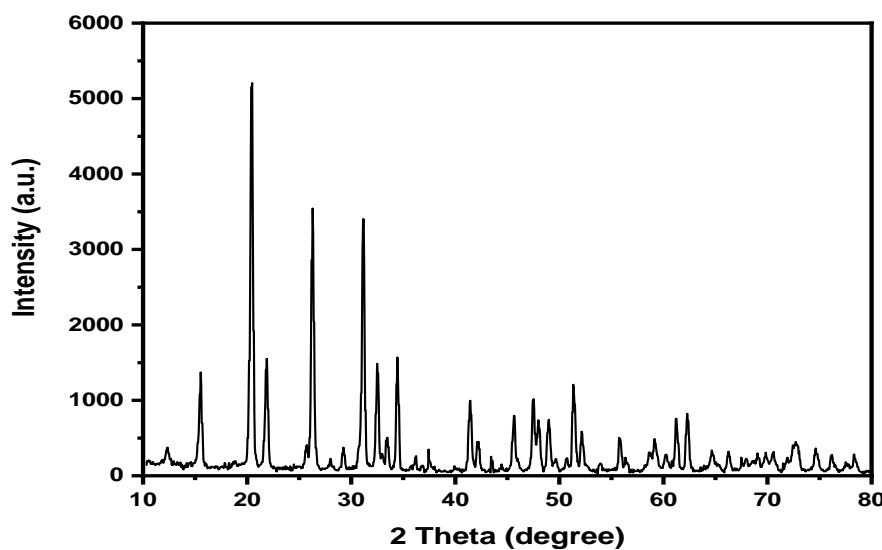


Figure 3. XRD of V₂O₅ Nps.

The average crystal size was calculated using the Debye Scherrer equation, which was discovered to be 34.39 nm in Table 1.

Table 1. The data of XRD for V₂O₅ Nps.

Pos. [°2Th.]	Height [cts]	FWHM [°2Th.]	Particle size (nm)	Average crystal size (nm)
15.5035	1075.66	0.1968	42.56	
20.4328	5096.82	0.2952	28.58	
21.8438	1358.53	0.2952	28.65	
25.6566	301.63	0.1968	43.27	
31.1647	3407.24	0.246	35.04	34.39
32.5534	1297.24	0.2952	29.30	
34.3961	1193.32	0.246	35.33	
42.1238	401.65	0.2952	30.14	
45.6724	765.53	0.246	36.63	
51.2964	815.49	0.2952	31.20	

EDX

The EDX spectrum Fig. 4, of V₂O₅ Nps, shows vanadium (V) and oxygen (O), showing their typical peaks in the spectrum. The results confirm

that the generated nanoparticles are highly pure. Additionally, the estimates obtained from the EDX measurement agree with the elemental theoretical computations¹⁴.

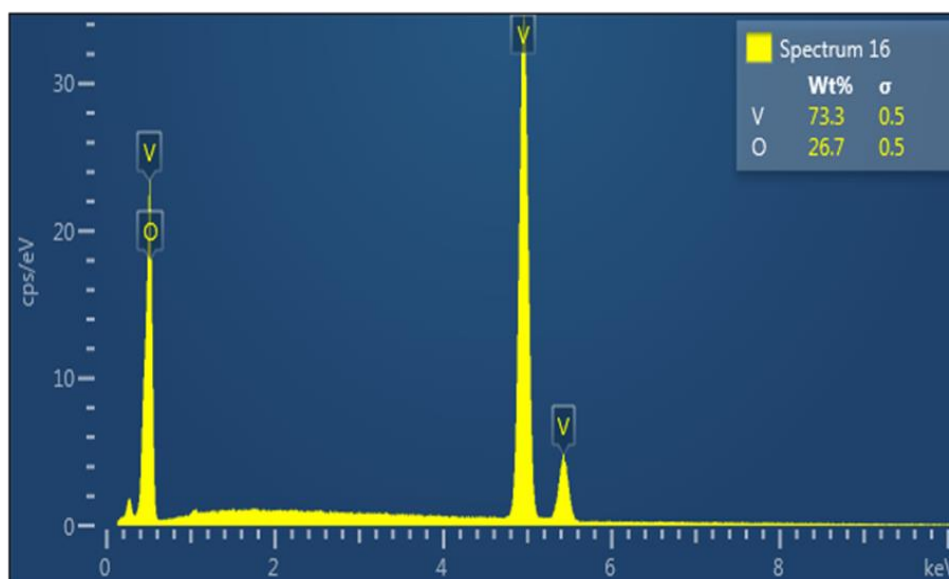


Figure 4. EDX of V₂O₅ Nps.

SEM and TEM

SEM and TEM images of V₂O₅ NPs clearly showed the nanostructured unconsolidated forms with low proportions of rods shown in Fig. 5 and 6. From the TEM image, the V₂O₅ nanoparticles appeared unconsolidated in a nanoscale form. It is also noted that there are high percentages of pores

in the samples, which distinguishes them in adsorption applications. From TEM image¹⁵, it has been concluded that the morphology of V₂O₅ nanoparticles was agglomerated together. The shape of the sample cannot be determined precisely due to the accuracy of the measurement. However, it seems to us that it contains measurements of the

spherical structure inside the sample, which are zero-dimensional (all its dimensions are within the

nanoscale), which is very preferred in surface chemistry for nanomaterials¹⁶.

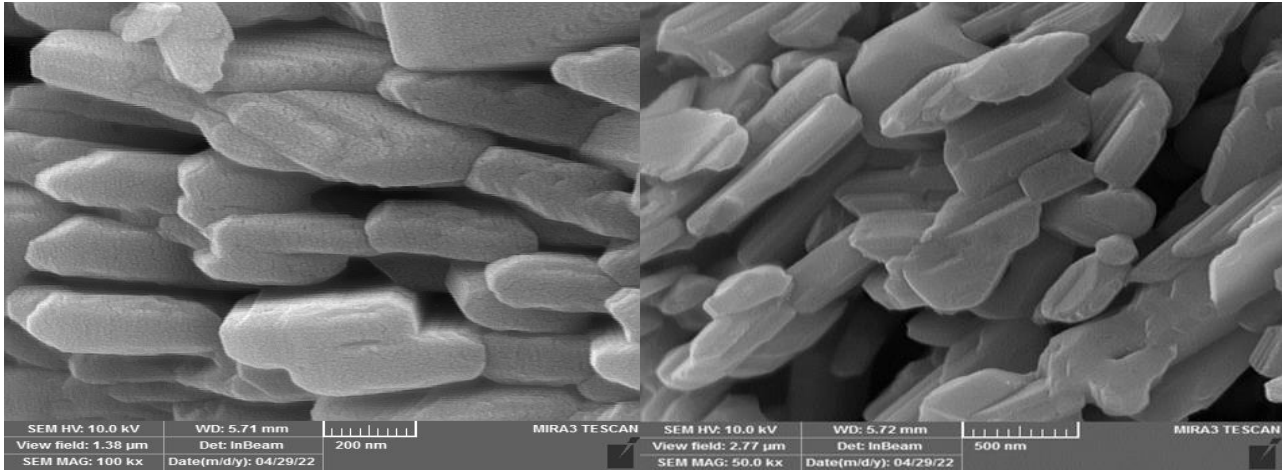


Figure 5. SE of V₂O₅ NPs.

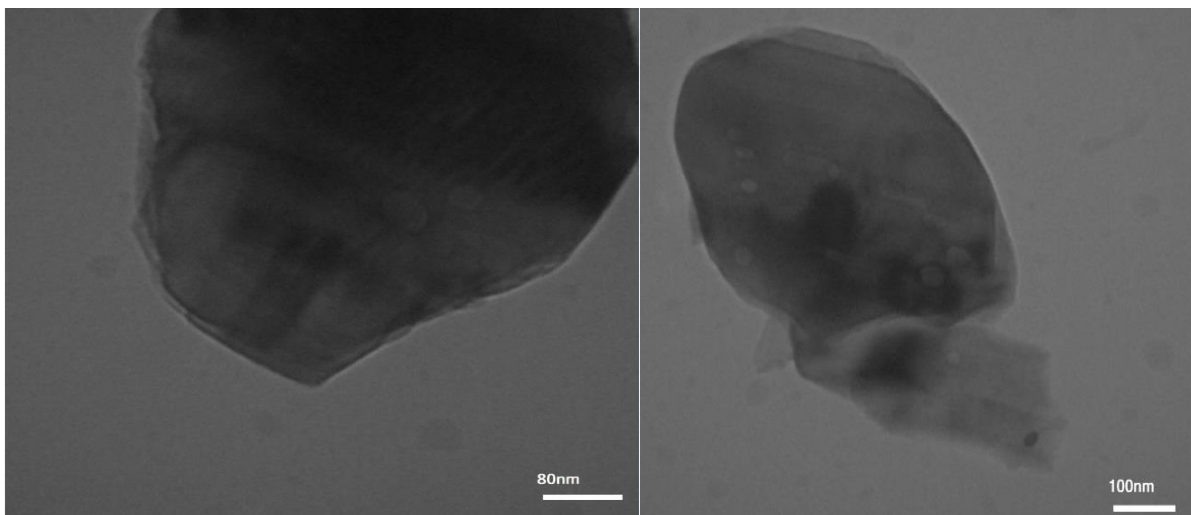


Figure 6. TEM of V₂O₅ Nps.

AFM

AFM surface analysis must be carefully examined since numerous factors, such as deformations or image artifacts resulting from a tip and contamination, might produce incorrect results. Whether to operate in contact or without contact is one of these crucial elements. The intensity of the surface contact between the tip and the sample, known as the contact mode, permanently damages V₂O₅ Nps nanoparticles. Since the tip is placed very close to the sample but not in contact with it, the non-contact mode is only required for this work.

After metallization, Fig. 7 depicts the creation of three-dimensional spherical clusters of V₂O₅ Nps in terms of optical behavior. The surface contains pores and high roughness and tends to the amorphous shape in the sample, which increases its porosity due to the green synthesis of the nanomaterial¹⁷⁻¹⁸. In the Height Accumulation Distribution Report of V₂O₅ NPs, we note that the size of the prepared oxide nanoparticles ranges between 10.00 and 20.00, which confirms that vanadium oxide prepared using pomegranate peel extract is a nano oxide¹⁹.

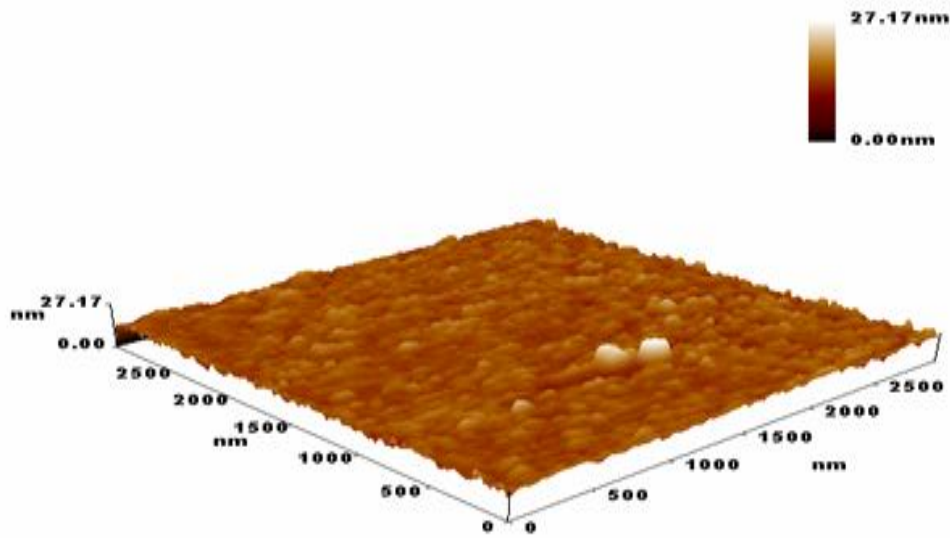


Figure 7. The AFM of V₂O₅ Nps.

Height Cumulation Distribution Report

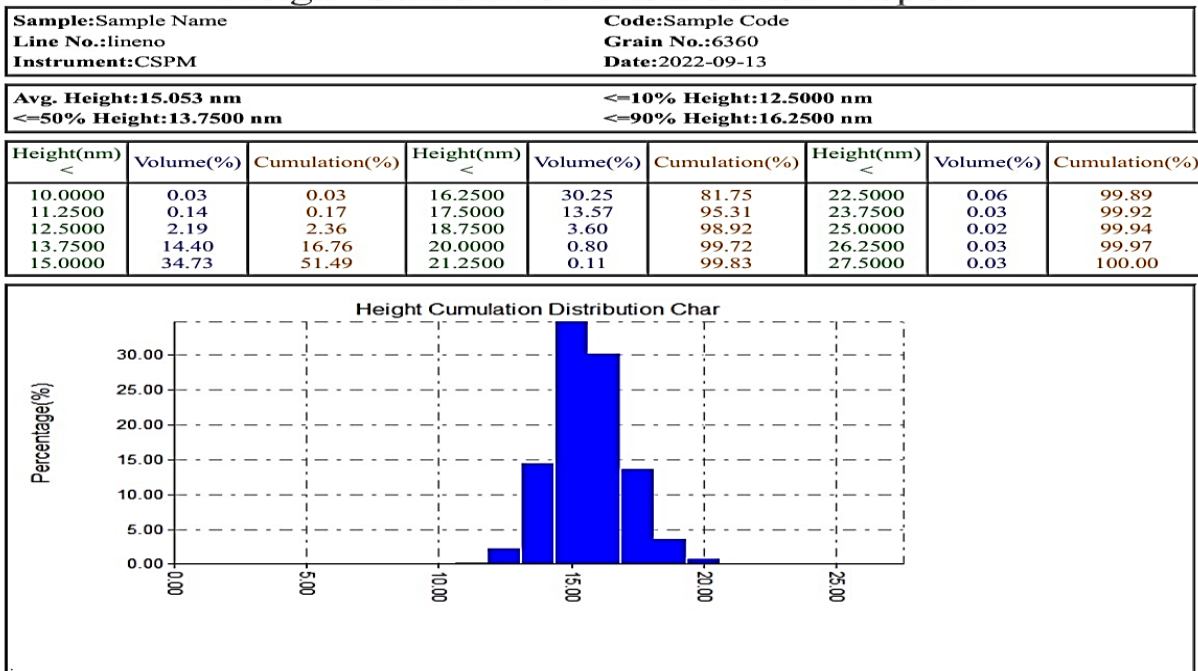


Figure 8. Height Cumulation Distribution Report.

Adsorption Studies

In comparing the adsorption behavior of the prepared metal oxide nanoparticles, the adsorption time profile was illustrated for each ion. Co (II) shows a continuous growth of the adsorption which means the process is far from equilibrium, and this behavior urges to suggest that this is not a simple type of adsorption; instead, it is a precipitation process in which metal oxide Nanoparticles act as

crystallization nuclei which initiate the crystallization of the cobalt chloride salt. For Ni (II) and Cu (II), the plateau of equilibrium is more apparent, especially for Ni (II) Fig. 9. The V₂O₅ surface is the largest one in an alternative form. This arrangement may be due to the convergences of the atomic radius of the V element with that of Adsorbate metal ions, which make them incorporate easily with active lattice sites of the metal oxide²⁰⁻²².

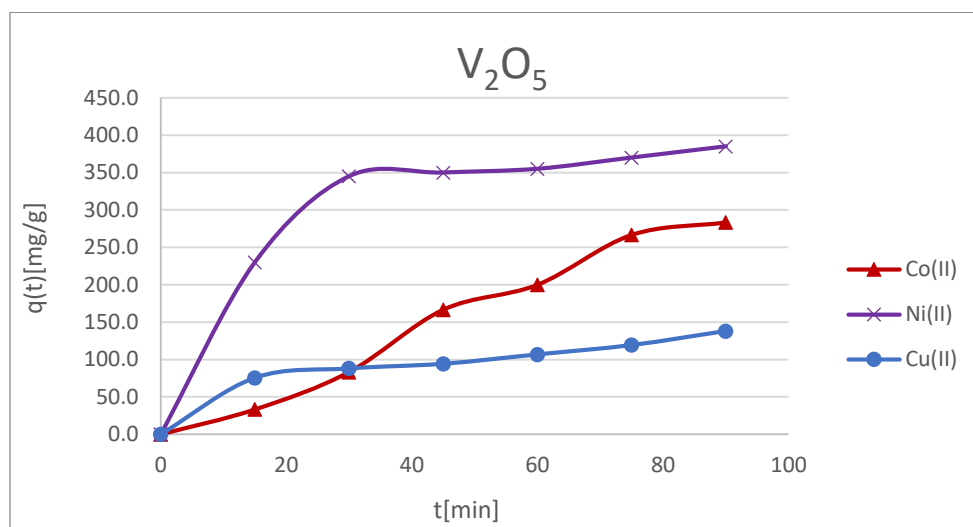


Figure 9. Adsorption time evolution of the metal ions on the V_2O_5 surfaces.

It is very clear from the above figures that the adsorption rate of Ni(II) is the highest one in the time scale and conditions of our experiment at all surfaces, while Co(ii) and Cu(II) ions are close in magnitude. The factors that affect the rate of the adsorption process are (i) charge, (ii) size, and (iii) electronic interactions. The first factor (charge) is the same in all ions, so it cannot be the significant factor that causes this difference. The size factor contributes to the diffusion process in the solution bulk and adsorbent mass as well²³, for these ions follow the order $Co(II) > Ni(II) > Cu(II)$. However, the variance is very small for bare ions. Considering the coordination and solvation shell, the difference will be negligible, especially in the solution. It will be considered after the initial adsorption in the diffusion stage in the metal oxide lattice and will take a different pattern. We think the electronic interaction factor is the primary important factor that causes this behavior. The magnetic moment of the unpaired electrons in the metal ions interacts with the magnetic moments of the unpaired electrons in the metal oxide. By this hypothesis, Co (II) must have the highest adsorption rate, followed by Ni (II) and then Cu (II). However, the observed decrease of the Co (II) adsorption rate and unlimited linear growth of the adsorbed portion indicate there is still another process taking place with the adsorption process, which is the Co (II) oxidation

by metal oxide²⁴⁻²⁶. The table below shows how to find the adsorption ratios for each ion on the surface of nano-vanadium oxide, which is equal to $(M+2 = Co, Ni, \text{ and } Cu)$ ions was 56.66%, 77.00%, and 27.23%.

Antimicrobial Studies

The agar well diffusion method was used to test the antibacterial activity of the produced V_2O_5 ²⁷ and V_2O_5 nanomaterial against the bacteria *E. coli*, *S. aureus*, and the fungus *Candida* in different concentrations of 25%, 50%, and 75%²⁸. The control as an antibiotic was streptomycin media, and the control was a DMSO solvent medium. The antimicrobial activities of the nanoplates were assessed by evaluating the zone of growth inhibition against the employed pathogens and adjusting the concentration of the manufactured V_2O_5 nanoplates. Concentrations of 75%, 50%, and 25% of V_2O_5 nanomaterial to demonstrate the antibacterial effectiveness of V_2O_5 nanomaterial in terms of zone of growth inhibition against the *E.coli*, *S. aureus* and the fungus *Candida* pathogens were the results of inhibition of vanadium oxide nanoparticles against positive and negative bacteria were compared with the standard drug Amoxicillin and the results of fungus inhibition with the standard drug Metronidazole. Shown in Tables 2,3 and Figs. 10,11.

Table 2. The zone inhibition of V₂O₅ NPs against different microbial.

Conc. mg/L	<i>Escherichia coli</i>	<i>Staphylococcus aureus</i>	<i>Candida albicans</i>
25	5	6	5
50	4	5	4
75	16	12	30

Table 3. The zone inhibition of drugs against different microbial at the highest concentration 75mg/L.

Sample	<i>Escherichia coli</i>	<i>Staphylococcus aureus</i>	<i>Candida albicans</i>
Amoxicillin	20	25	--
Metronidazol	--	--	35

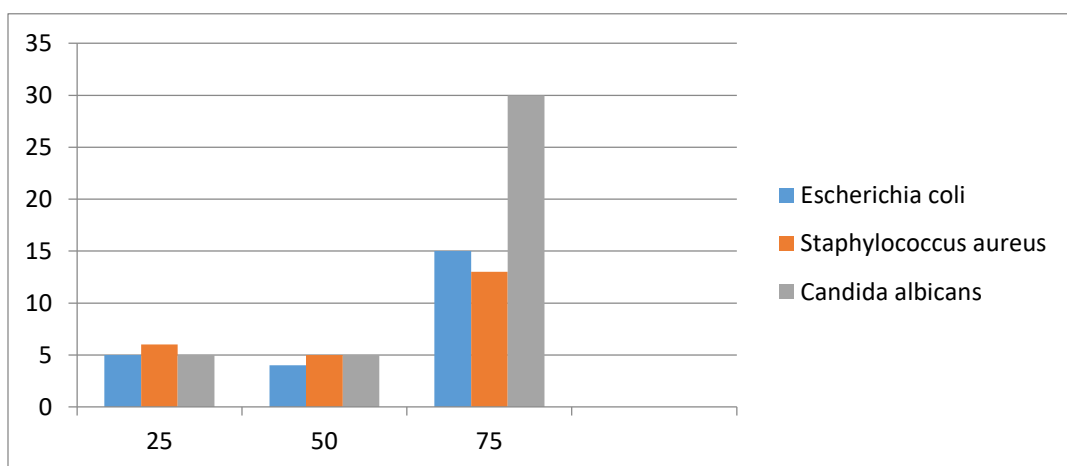


Figure 10. The antibacterial activity of V₂O₅ NPs.

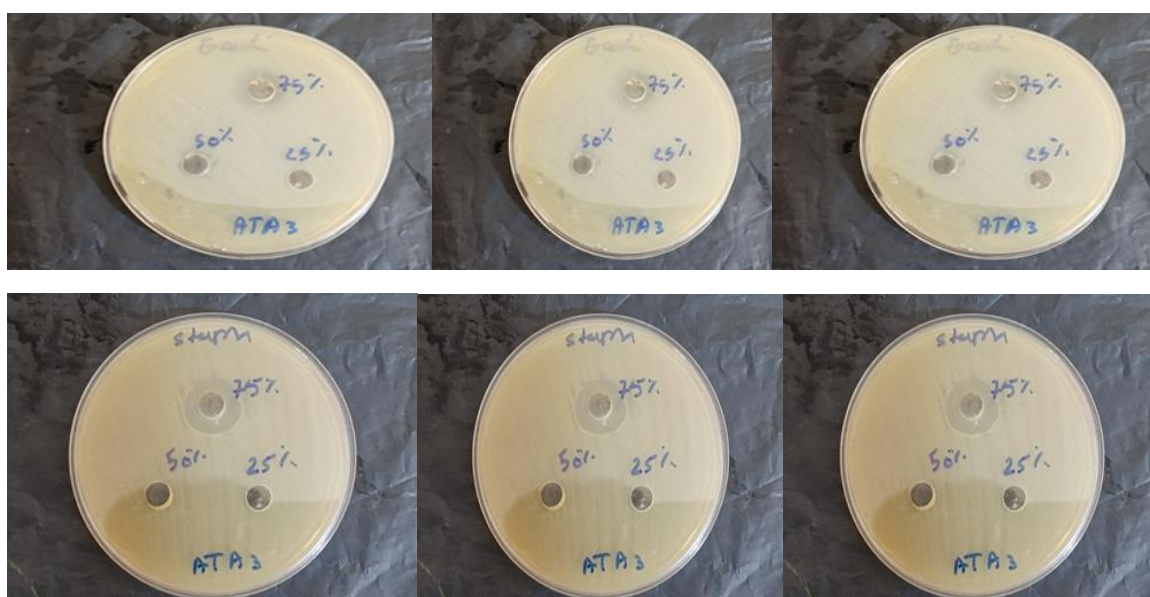


Figure 11. Zone of growth inhibition against *E.coli* and *S. aureus*.

Conclusion

V₂O₅NPs were synthesized by the biosynthesis method of V₂O₅NPs rhombohedra phase with a diameter (34.39) nm obtained using VOSO₄.H₂O. The morphology of V₂O₅NPs was as an aggregation of thin sheet clusters. They have antimicrobial

activity inhibiting the growth of *S. aureus*, *E. coli*, and a very high inhibition with *Candida albicans* fungal. V₂O₅NPs were removed simultaneously with three metal ions (M⁺² = Co, Ni, and Cu) from water contaminated with them.

Acknowledgment

The author states their truthful appreciations to Chemistry Department, College of Education for

Pure Sciences in Ibn-Al Haitham, University in Baghdad, Iraq for the fiscal support of this study.

Authors' Declaration

- Conflicts of Interest: None.
- We hereby confirm that all the Figures and Tables in the manuscript are ours. Furthermore, any Figures and images, that are not ours, have been included with the necessary permission for

re-publication, which is attached to the manuscript.

- Ethical Clearance: The project was approved by the local ethical committee in University of Baghdad.

Authors' Contribution Statement

A. T. A. and L. K. A. K. certify that we have participated title of MS (Biosynthesis, Characterization, Adsorption and Antimicrobial study of Vanadium Oxide Nanoparticles Using

Punica Granatum Extract) in different roles as follows: Conception, design, acquisition of data, analysis, interpretation, drafting the MS, revision and proofreading.

References

1. Marozzi S, Sabouri Z, Darroudi M. Greener synthesis and medical applications of metal oxide nanoparticles. *Ceram Int.* 2021 Jul 15; 47(14): 19632-50. <https://doi.org/10.1016/j.ceramint.2021.03.301>
2. Turan NB, Erkan HS, Engin GO, Bilgili MS. Nanoparticles in the aquatic environment: Usage, properties, transformation, and toxicity. *Process Saf Environ.* 2019 Oct 1; 130: 238-49. <https://doi.org/10.1016/j.psep.2019.08.014>
3. Thakur P, Thakur A. Introduction to Nanotechnology. In *Synthesis and Applications of Nanoparticles 2022*; 459: 1-17. Springer, SG. https://doi.org/10.1007/978-981-16-6819-7_1
4. Bukhari A, Ijaz I, Gilani E, Nazir A, Zain H, Saeed R, *et al.* Green synthesis of metal and metal oxide nanoparticles using different plants' parts for antimicrobial activity and anticancer activity. *Coatings.* 2021 Nov 9; 11(11): 1374. <https://doi.org/10.3390/coatings11111374>
5. Lashari A, Hassan SM, Mughal SS. Biosynthesis, Characterization and Biological Applications of BaO Nanoparticles using *Linum usitatissimum*. *Am J Appl. Sci.* 2022; 8(3): 58-68. <https://doi.org/10.11648/j.ajasr.20220803.14>
6. Diniz MO, Golin AF, Santos MC, Bianchi RF, Guerra EM. Improving the performance of polymer-based ammonia gas sensor using POMA/V₂O₅ hybrid films. *Org Electron.* 2019 Apr 1; 67: 215-21. <https://doi.org/10.1016/j.orgel.2019.01.039>
7. Dadkhah M, Tulliani JM. Green synthesis of metal oxides semiconductors for gas sensing applications. *Sensors.* 2022 Jun 21; 22(13): 4669. <https://doi.org/10.3390/s22134669>
8. Niño-Martínez N, Salas Orozco MF, Martínez-Castañón GA, Torres Méndez F, Ruiz F. Molecular mechanisms of bacterial resistance to metal and metal oxide nanoparticles. *Int J Mol Sci.* 2019 Jun 8; 20(11): 2808. <https://doi.org/10.3390/ijms20112808>
9. Yu Z, Li Q, Wang J, Yu Y, Wang Y, Zhou Q, *et al.* Reactive oxygen species-related nanoparticle toxicity in the biomedical field. *Nanoscale Res Lett.* 2020 Dec; 15(1): 1-4. <https://doi.org/10.1186/s11671-020-03344-7>
10. Boretti A, Rosa L. Reassessing the projections of the world water development report. *NPJ Clean Water.*

- 2019 Jul 31; 2(1): 1-6.
<https://doi.org/10.1038/s41545-019-0039-9>.
11. Gusain R, Gupta K, Joshi P, Khatri OP. Adsorptive removal and photocatalytic degradation of organic pollutants using metal oxides and their composites: A comprehensive review. *Adv Colloid Interface Sci.* 2019 Oct 1; 272: 102009.
<https://doi.org/10.1016/j.cis.2019.102009>.
12. Shvets P, Dikaya O, Maksimova K, Goikhman A. A review of Raman spectroscopy of vanadium oxides. *Adv Colloid Interface Sc.* 2019 Aug; 50(8): 1226-44.
<https://doi.org/10.1002/jrs.5616>.
13. Baster D, Kondracki Ł, Oveisi E, Trabesinger S, Girault HH. Prussian Blue Analogue—Sodium—Vanadium Hexacyanoferrate as a Cathode Material for Na-Ion Batteries. *ACS Appl Energy Mater.* 2021 Sep 1; 4(9): 9758-65.
<https://doi.org/10.1021/acsaem.1c01832>.
14. Subramanian M, Dhayabaran VV, Shanmugavadeivel M. Room temperature fiber optic gas sensor technology based on nanocrystalline Ba₃(VO₄)₂: Design, spectral and surface science. *Mater Res Bull.* 2019 Nov 1; 119: 110560.
<https://doi.org/10.1016/j.materresbull.2019.110560>.
15. Al Jabbar JL, Apriandanu DO, Yulizar Y, Sudirman S. Synthesis, characterization and catalytic activity of V₂O₅ nanoparticles using *Foeniculum vulgare* stem extract. *IOP Conf. Ser: Mater Sci Eng.* 2020 Feb 1; 763 (1): 012031. IOP Publishing. <https://doi.org/10.1088/1757-899X/763/1/012031>.
16. Peng J, Guo J, Ma R, Jiang Y. Water-solid interfaces probed by high-resolution atomic force microscopy. *Surf Sci Rep.* 2021 Nov 20: 100549.
<https://doi.org/10.1016/j.surfrep.2021.100549>.
17. Karimi F Ayati A, Tanhaei B, Sanati AL, Afshar S, Kardan A, Dabirifar Z, Karaman C. Removal of metal ions using a new magnetic chitosan nano-bio-adsorbent; A powerful approach in water treatment. *Environ Res.* 2022 Jan 1; 203: 111753.
<https://doi.org/10.1016/j.envres.2021.111753>.
18. Almomani F, Bhosale R, Khraisheh M, Almomani T. Heavy metal ions removal from industrial wastewater using magnetic nanoparticles (MNP). *Appl Surf Sci.* 2020 Mar 15; 506: 144924.
<https://doi.org/10.1016/j.apsusc.2019.144924>.
19. Gautam S, Kumar A, Vashistha VK, Das DK. Phyto-assisted synthesis and characterization of V₂O₅ nanomaterial and their electrochemical and antimicrobial investigations. *Nano Life.* 2020 Sep 3; 10(03): 2050003.
<https://doi.org/10.1142/S1793984420500038>.
20. Amer AA, Karem LK. Biological Evaluation and Antioxidant Studies of NiO, Pdo and Pt Nanoparticles Synthesized from a New Schiff Base Complexes. *Ibn al-Haitham J Pure Appl Sci.* 2022; 35(4): 170-182.
<https://doi.org/10.30526/35.4.2864>.
21. Sadiq Khasro F, Mahmood HS. Enhancement of Antibacterial Activity of Face Mask with Gold Nanoparticles. *Ibn al-Haitham J Pure Appl Sci.* 2022 Jul 20; 35(3): 25-31.
<https://doi.org/10.30526/35.3.2844>.
22. Baqer SR., Alsammarrarie AM A, Alias M, Al-Halbosiy MM, Sadiq AS. In Vitro Cytotoxicity Study of Pt Nanoparticles Decorated TiO₂ Nanotube Array. *Baghdad Sci J.* 2020; 17(4): 1169-1169.
<https://doi.org/10.21123/bsj.2020.17.4.1169>
23. Ali AH, Shakir ZH, Mazher AN, Mazhir SN. Influence of Cold Plasma on Sesame Paste and the Nano Sesame Paste Based on Co-occurrence Matrix. *Baghdad Sci J.* 2022; 19(4): 855-864.
<https://doi.org/10.21123/bsj.2022.19.4.0855>.
24. Shanan ZJ, Majed MD, Ali HM. Effect of the Concentration of Copper on the Properties of Copper Sulfide Nanostructure. *Baghdad Sci J.* 2022; 19(1): 225-232.
<https://doi.org/10.21123/bsj.2022.19.1.0225>.
25. Alwan Al Mashhadani AM, Himdan TA, Hamadi Al Dulaimi AS, M AbuZaid YI. Adsorptive removal of some carbonyl-containing compounds from aqueous solutions using Iraqi porcelanite rocks: a kinetic-model study. *Caps J Environ Sci.* 2022 Jan 1; 20(1): 117-29. <https://doi.org/10.22124/cjes.2022.5406>
26. ZHANG, Xiaoyuan; LIU, Yu. Concurrent removal of Cu (II), Co (II) and Ni (II) from wastewater by nanostructured layered sodium vanadosilicate: Competitive adsorption kinetics and mechanisms. *J Environ Chem Eng.* 2021; 9(5): 105945.
<https://doi.org/10.1016/j.jece.2021.105945>
27. Sridhar, Chakradhar, Nagesh Gunvanthrao Yernale, and M. V. N. Prasad. Synthesis, spectral characterization, and antibacterial and antifungal studies of PANI/V₂O₅ nanocomposites. *Int J Chem Eng Res.* 2016; (2016): 1-6.
<https://doi.org/10.1155/2016/3479248>
28. Mohammed SS, Aziz NM, Abdul Karem LK. Preparation and Diagnostics of Schiff Base Complexes and Thermodynamic Study for Adsorption of Cobalt Complex on Iraqi Attapulgit Clay Surface. *Egypt J Chem.* 2021 Dec 1; 64(12): 2-3. <https://doi.org/10.21608/ejchem.2021.75540.3703>.

التحضير الحيوي والتشخيص ودراسات الامتزاز ومضاد الميكروبات لجسيمات اوكسيد الفناديوم النانوية باستخدام مستخلص قشور الرمان

انغام طارق علي¹، لقاء خالد عبد الكريم²

قسم الكيمياء، كلية التربية للعلوم الصرفة ابن الهيثم، جامعة بغداد، بغداد، العراق.

الخلاصة

تتضمن هذه الدراسة استخدام التكنولوجيا الصديقة للبيئة أو التخليق الحيوي ، والتي تعتبر فعالة من حيث التكلفة المنخفضة وقلة الوقت والطاقة لتحضير الجسيمات النانوية V_2O_5NPs من كبريتات الفناديوم $VSO_4.H_2O$ باستخدام المستخلص المائي لقشور الرمان Punica Granatum في وسط قاعدي باستخدام هيدروكسيد الصوديوم بتركيز (0.1M) وتتراوح قيمة PHI لوسط التفاعل من 8-12. تم تشخيص الجسيمات النانوية V_2O_5NPs باستخدام عدة تقنيات ، مثل FT-IR ، الأشعة فوق البنفسجية- المرئية بفجوة الطاقة $E_g = 3.734eV$ ، تم حساب XRD حيود الأشعة السينية باستخدام معادلة Debye Scherres ، والتي من خلالها تم التوصل الى ان معدل حجم حبيبات اوكسيد الفناديوم النانوي هي 34.39. كما تم استخدام المجهر الالكتروني الماسح SEM والمجهر الالكتروني النافذ TEM كما تم تحديد حجم وهيكل وتكوين V_2O_5NPs المحضر باستخدام تقنيه (EDX) والتي بينت نسبه عنصر الفناديوم ونسبة عنصر الاوكسجين في المركب مما يثبت تكون اوكسيد الفناديوم ، وباستخدام مجهر القوة الذرية AFM تبين ان حجمها يتراوح بين 10- 20nm. وهذا يدل ان الاوكسيد المحضر نانوي. كفاءة الامتزاز للايونات الفلزات (II) M مثل Ni و Co و Cu عند طول الموجي الاعظم λ_{max} (510 ، 425 ، 814) نانومتر كانت 56.66% و 77.00% و 27.23% على التوالي. تم اختبار النشاط المضاد للبكتريا لـ V_2O_5NPs بثلاثة تركيز 25% و 50% و 75% ضد بكتريا موجبة *Escherichia coli* وواخرى سالبة *Staphylococcus aureus* و فطر *Candida albicans* تمت مقارنة نتائج تثبيط اوكسيد الفناديوم النانوي تجاه انواع البكتريا السالبة والموجبة مع الدواء القياسي Amoxicillin ونتائج تثبيط الفطر مع الدواء القياسي Metronidazole وتبين ان الاوكسيد النانوي يكون اكثر فعالية عند التركيز 75%.

الكلمات المفتاحية: امتزاز، مضاد الميكروبات ، تحضير الحيوي ، قشور الرمان، ازالة.